Resonant scattering properties close to a *p*-wave Feshbach resonance

F. Chevy,[1] E. G. M. van Kempen,[2] T. Bourdel,[1] J. Zhang,[3] L. Khaykovich,[4] M. Teichmann,[1] L. Tarruell,[1]
S. J. J. M. F. Kokkelmans,[2] and C. Salomon[1]

[1]*Laboratoire Kastler-Brossel, ENS, 24 rue Lhomond, 75005 Paris*
[2]*Eindhoven University of Technology, P. O. Box 513, 5600 MB Eindhoven, The Netherlands*
[3]*SKLQOQOD, Institute of Opto-Electronics, Shanxi University, Taiyuan 030006, People's Republic of China*
[4]*Department of Physics, Bar Ilan University, Ramat Gan 52900, Israel*

We present a semianalytical treatment of both the elastic and inelastic collisional properties near a *p*-wave Feshbach resonance. Our model is based on a simple three-channel system that reproduces more elaborate coupled-channel calculations. We stress the main differences between *s*-wave and *p*-wave scattering. We show in particular that, for elastic and inelastic scattering close to a *p*-wave Feshbach resonance, resonant processes dominate over the low-energy behavior.

I. INTRODUCTION

The observation of molecular gaseous Bose-Einstein condensates (BECS) and the subsequent experimental study of the BEC-BCS crossover [1–5] were made possible by the possibility of tuning interatomic interactions using a magnetic field (the so-called Feshbach resonances). Although all these experiments were based on *s*-wave interatomic interactions, it is known from condensed matter physics that superfluidity of fermionic systems can also arise through higher-order partial waves. The most famous examples of this nonconventionnal superfluidity are ^{3}He [6], for which the Cooper pairs spawn from *p*-wave interactions, and high-T_c superconductivity, in which pairs are known to possess *d*-wave symmetry [7]. Recent interest in *p*-wave interactions in cold atom gases stemmed from these possibilities and resulted in the observation of *p*-wave Feshbach resonances in ^{40}K [8] and ^{6}Li [9,10], as well as theoretical studies on the superfluidity of cold atoms interacting through *p*-wave pairing [11,12].

The present paper is devoted to the study of *p*-wave interactions close to a Feshbach resonance and it derives some results presented in [9]. In a first part, we present the model we use to describe both elastic and inelastic processes that are discussed in the second part. We stress in particular the main qualitative differences between *p*-wave and *s*-wave physics and show that contrarily to the case of the *s* wave, which is dominated by low-energy physics, *p*-wave scattering is dominated by a resonance peak associated to the quasibound molecular state. Finally, we compare our analytical results to numerical coupled-channel calculations.

II. MODEL FOR *p*-WAVE INTERACTIONS

We consider the scattering of two identical particles of mass m. As usual when treating a two-body problem, we work in the center-of-mass frame and consider only the motion of a fictitious particle of mass $m/2$ interacting with a static potential. In order to study the *p*-wave Feshbach resonance, we use a model based on the separation of open and closed channels. In this framework, the Feshbach resonance arises in an open channel as a result of the coupling with a closed channel [13]. At resonance, scattering properties are dominated by resonant effects and we can neglect all "background" scattering (i.e., we assume there is no scattering far from resonance).

(1) We restrict ourselves to a three-channel system, labeled 1, 2, and 3, which correspond to the different two-body spin configurations (Fig. 1). Channels $|1\rangle$ and $|2\rangle$ are open channels. We focus on the situation where atoms are prepared initially in state $|1\rangle$. Atoms may be transferred to state $|2\rangle$ after an inelastic process. Channel $|3\rangle$ is closed and hosts the bound state leading to the Feshbach resonance.

Let us consider, for instance, the case of ^{6}Li atoms prepared in a mixture of $|F=1/2, m_F=1/2\rangle$ and $|F'=1/2, m'_F=-1/2\rangle$. In this system, the only two-body decay channel is associated with the flipping of an $m_F=-1/2$ atom to $m_F=1/2$. If we denote by (m_F, m'_F) the symmetrized linear combination of the states $|F=1/2, m_F\rangle$ and $|F'=1/2, m'_F\rangle$, then $|1\rangle=(1/2,-1/2)$ and $|2\rangle=(1/2,1/2)$.
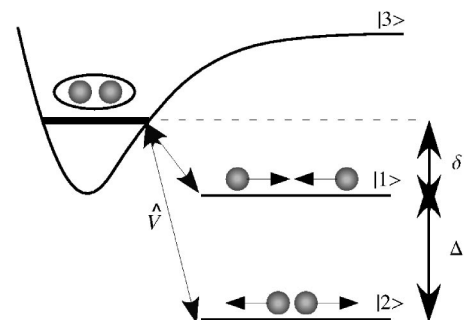

FIG. 1. The *p*-wave model: we consider three internal states, labeled $|1\rangle$, $|2\rangle$, and $|3\rangle$. States $|1\rangle$ and $|2\rangle$ are two open channels corresponding, respectively, to the incoming and decay channels. The released energy in an inelastic collision bringing an atom initially in $|1\rangle$ to $|2\rangle$ is denoted Δ. State $|3\rangle$ is a closed channel that possesses a *p*-wave bound state of energy δ nearly resonant with state $|1\rangle$. Finally, we assume that these three channels interact through a potential $\hat{V}$ acting only on the internal states and coupling the two open channels to the closed channel.

(2) The Feshbach resonances studied here are all located at values of the magnetic field where the Zeeman splitting is much larger than the hyperfine structure. In a first approximation we can therefore assume that the internal states are described by uncoupled electronic and nuclear spin states. In the absence of any dipolar or hyperfine coupling between the electronic singlet and triplet manifolds, we assume we have no direct interaction in channels 1 and 2 so that the eigenstates are plane waves characterized by their relative wave vector k and their energy $E_1(k) = \hbar^2 k^2/m$ (channel 1) and $E_2(k) = -\Delta + \hbar^2 k^2/m$ (channel 2). $\Delta > 0$ is the energy released in an inelastic process leading from 1 to 2. Δ can be considered as independent of the magnetic field and is assumed to be much larger than any other energy scales (in the case relevant to our experiments, $\Delta/h \sim 80$ MHz is the hyperfine splitting of ^{6}Li at high field).

(3) In channel 3, we consider only a p-wave bound state nesting at an energy δ quasiresonant with channel 1. In the case of ^{6}Li atoms in the $F = 1/2$ hyperfine state, $\delta = 2\mu_B(B - B_0)$, where B is the magnetic field and B_0 is the position of the "bare" Feshbach resonance. If the projection of the angular momentum (in units of $\hbar$) is denoted by $m_{\mathbf{u}}$ for a quantization axis chosen along some vector $\mathbf{u}$, the eigenfunctions associated with this bound state can be written as $g(r)Y_1^{m_{\mathbf{u}}}(\theta, \phi)$, where (r, θ, ϕ) is the set of polar coordinates and the Y_l^m are the spherical harmonics.

(4) The coupling $\hat{V}$ between the various channels affects only the spin degrees of freedom. Therefore the orbital angular momentum is conserved during the scattering process and we restrict our analysis to the p-wave manifold. This is in contrast to the situation in heavy alkalimetals where incoming particles in the s wave can be coupled to molecular states of higher orbital angular momentum [14,15].

We assume also that the only nonvanishing matrix elements are between the closed and the open channels (i.e., $\langle 1,2|\hat{V}||3\rangle$ and $\langle 3|\hat{V}|1,2\rangle$).

Let us denote a state of the system by $|\alpha, \chi\rangle$, where $\alpha \in \{1,2,3\}$ and χ describe, respectively, the internal (spin) and the orbital degrees of freedom. According to assumption ((4)), the matrix element $\langle \alpha, \chi|\hat{V}|\alpha', \chi'\rangle$ is simply given by

$$\langle \alpha, \chi|\hat{V}|\alpha', \chi'\rangle = \langle \chi|\chi'\rangle \langle \alpha|\hat{V}|\alpha'\rangle, \tag{1}$$

and is therefore simply proportional to the overlap $\langle \chi|\chi'\rangle$ between the external states.

Let us now particularize to the case where $\alpha \in \{1,2\}$, and $|\chi\rangle = |\mathbf{k}\rangle$ is associated with a plane wave of relative momentum $\hbar\mathbf{k}$. According to hypothesis ((4)), this state is coupled only to the closed channel $|3\rangle$. Moreover, using the well-known formula $e^{ikz} = \Sigma_l i^l \sqrt{4\pi(2l+1)} j_l(kr) Y_l^0(\theta, \phi)$, where the j_l are the spherical Bessel functions, we see that $|\chi\rangle$ is coupled only to the state $|\alpha' = 3, \mathbf{k} = \mathbf{0}\rangle$ describing the pair in the bound state $|\alpha' = 3\rangle$ with zero angular momentum in the $\mathbf{k}$ direction. The matrix element then reads
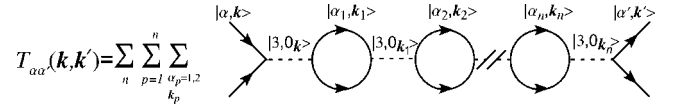

FIG. 2. Diagrammatic expansion of the T matrix. The full (dashed) lines represent free atoms (molecules). $|\alpha, \mathbf{k}\rangle$ is the scattering state of the two particles, in the internal state $\alpha = 1, 2$. $|3, 0_{\mathbf{k}}\rangle$ represents the state of a p-wave molecule with orbital angular momentum component zero on the $\mathbf{k}$ direction.

$$\langle \alpha, \mathbf{k}|\hat{V}|3, m_{\mathbf{k}}\rangle = i\delta_{m_{\mathbf{k}},0} \sqrt{\frac{12\pi}{L^3}} \langle \alpha|\hat{V}|3\rangle \int g^*(r) j_1(kr) r^2 dr, \tag{2}$$

where L^3 is a quantization volume. Since for small k we have $j_1(kr) \sim kr/3$, the matrix element $\langle \alpha, \mathbf{k}|\hat{V}|3, m_{\mathbf{k}}\rangle$ takes the general form

$$\langle \alpha, \mathbf{k}|\hat{V}|3, m_{\mathbf{k}}\rangle = \delta_{m_{\mathbf{k}},0} \frac{kF_\alpha(k)}{\sqrt{L^3}}, \tag{3}$$

where $F_\alpha(k)$ has a finite (in general nonzero) limit when k goes to zero.

Later on, we shall also need the coupling between $|\alpha, \mathbf{k}\rangle$ and $|3, m_{\mathbf{k}'} = 0\rangle$ (that will be denoted by $|3, 0_{\mathbf{k}'}\rangle$), where the momentum $\mathbf{k}$ and the direction of quantization $\mathbf{k}'$ are no longer parallel. The calculation presented above yields readily

$$\langle \alpha, \mathbf{k}|\hat{V}|3, 0_{\mathbf{k}'}\rangle = \frac{kF_\alpha(k)}{\sqrt{L^3}} \langle 0_{\mathbf{k}}|0_{\mathbf{k}'}\rangle = \frac{kF_\alpha(k)}{\sqrt{L^3}} \cos(\widehat{\mathbf{k}, \mathbf{k}'}), \tag{4}$$

where $(\widehat{\mathbf{k}, \mathbf{k}'})$ is the angle between $\mathbf{k}$ and $\mathbf{k}'$ [16].

III. T MATRIX

From general quantum theory, it is known that the scattering properties of a system are given by the so-called T matrix $\hat{T}$. It can be shown in particular that $\hat{T}$ is given by the following expansion in powers of the coupling potential:

$$\hat{T}(E) = \hat{V} + \hat{V}\hat{G}_0(E)\hat{V} + \hat{V}\hat{G}_0(E)\hat{V}\hat{G}_0(E)\hat{V} + \cdots, \tag{5}$$

where $\hat{G}_0(E) = 1/(E - \hat{H}_0)$ and $\hat{H}_0 = \hat{H} - \hat{V}$ is the free Hamiltonian of the system.

Let us consider $|\alpha, \mathbf{k}\rangle$ and $|\alpha', \mathbf{k}'\rangle$, two states of the *open channels*, and let us set $T_{\alpha\alpha'}(\mathbf{k}, \mathbf{k}', E) = \langle \alpha, \mathbf{k}|\hat{T}(E)|\alpha', \mathbf{k}'\rangle$. According to formula (5), this matrix element is the sum of terms that can be represented by the diagram of Fig. 2 and we get after a straightforward calculation

$$T_{\alpha\alpha'}(\mathbf{k}, \mathbf{k}', E) = \frac{kk'}{L^3} F_\alpha(k) F_{\alpha'}^*(k') \sum_{n=0}^{\infty} R_n \Lambda(E)^n G_0^{(m)}(E)^{n+1}.$$

Here $G_0^{(m)}(E) = 1/(E - \delta)$ is the free propagator for the molecule, $\Lambda = \Lambda_1 + \Lambda_2$ with

$$\Lambda_\alpha(E) = \int \frac{q^4 dq}{(2\pi)^3} \frac{|F_\alpha(q)|^2}{E - E_\alpha(q)} \qquad (6)$$

the results of the integration on the loops, and finally

$$R_n = \int d^2\Omega_1 \cdots d^2\Omega_n \cos(\widehat{\mathbf{k},\mathbf{k}_1})$$

$$\times \cos(\widehat{\mathbf{k}_1,\mathbf{k}_2}) \cdots \cos\widehat{\mathbf{k}_n,\mathbf{k}'},$$

where Ω_p is the solid angle associated with $\mathbf{k}_p$, arises from the pair-breaking vertices $|3, 0_{\mathbf{k}_i}\rangle \to |\alpha_{i+1}, \mathbf{k}_{i+1}\rangle$. This last integral can be calculated recursively and we get R_n $= (4\pi/3)^n \cos(\widehat{\mathbf{k},\mathbf{k}'})$, that is, for the T matrix

$$T_{\alpha\alpha'}(\mathbf{k},\mathbf{k}',E) = \frac{1}{L^3} \frac{kk' F_\alpha(k) F_{\alpha'}^*(k')}{E - \delta - \Sigma_1 - \Sigma_2} \cos(\widehat{\mathbf{k},\mathbf{k}'}),$$

with $\Sigma_\alpha = 4\pi\Lambda_\alpha/3$.

This expression can be further simplified since, according to Eq. (2), the width of $F_\alpha(q)$ is of the order of $1/R_e$, where R_e is the characteristic size of the resonant bound state. In the low-temperature limit, we can therefore expand Σ_α with the small parameter kR_e.

From Eq. (2), we see that replacing $F_\alpha(q)$ by its value at $q=0$ leads to a q^2 divergence. This divergence can be regularized by the use of counterterms in the integral, namely, by writing that

$$\Sigma_\alpha(E) = \int |F_\alpha(q)|^2 \left[\frac{q^4}{E - E_\alpha(q)} + \frac{mq^2}{\hbar^2} + \frac{m^2}{\hbar^4}[E - E_\alpha(0)] \right] \frac{dq}{6\pi^2}$$

$$- \int |F_\alpha(q)|^2 \frac{mq^2}{\hbar^2} \frac{dq}{6\pi^2}$$

$$- [E - E_\alpha(0)] \int |F_\alpha(q)|^2 \frac{m^2}{\hbar^4} \frac{dq}{6\pi^2},$$

where we have assumed that F_α was decreasing fast enough at large q to ensure the convergence of the integrals. $|F_\alpha(q)|^2$ can now be safely replaced by $\lambda_\alpha = |F_\alpha(0)|^2$ in the first integral and we finally get

$$\Sigma_\alpha = -i\frac{\lambda_\alpha}{6\pi}\frac{m}{\hbar^2}\left(\frac{m}{\hbar^2}[E - E_\alpha(0)]\right)^{3/2} - \delta_{0,\alpha} - \eta_\alpha[E - E_\alpha(0)],$$

with

$$\delta_0^{(\alpha)} = \int |F_\alpha(q)|^2 \frac{mq^2}{\hbar^2} \frac{dq}{6\pi^2},$$

$$\eta_\alpha = \int |F_\alpha(q)|^2 \frac{m^2}{\hbar^4} \frac{dq}{6\pi^2}.$$

If we assume that the release energy Δ is much larger than E and if we set $\delta_0 = \delta_0^{(1)} + \delta_0^{(2)}$ and $\eta = \eta_1 + \eta_2$, we get for the T matrix

$$T_{\alpha\alpha'}(\mathbf{k},\mathbf{k}',E) \simeq \frac{1}{L^3} \frac{kk' F_\alpha(0) F_{\alpha'}^*(0)\cos(\widehat{\mathbf{k},\mathbf{k}'})/(1+\eta)}{E - \tilde\delta + i\hbar\gamma(E)/2} \qquad (7)$$

with

$$\hbar\gamma(E) = \left(\frac{m}{\hbar^2}\right)^{5/2} \frac{(\lambda_2 \Delta^{3/2} + \lambda_1 E^{3/2})}{3\pi(1+\eta)},$$

$$\tilde\delta = \frac{(\delta - \delta_0)}{1 + \eta}.$$

We note that this expression for the T matrix is consistent with the general theory of multichannel scattering resonances [13], where resonantly enhanced transitions to other channels are readily included. In a similar context of two open channels and a Feshbach resonance, a recent experiment was analyzed [15] that involved the decay of a molecular state formed from a Bose-Einstein condensate.

IV. *s* WAVE VS *p* WAVE

This section is devoted to the discussion of the expression found for the T matrix. In addition to the scattering cross section, the study of the T matrix yields important information on the structure of the dressed molecular state underlying the Feshbach resonance and we will demonstrate important qualitative differences between the behaviors of *p*-wave and *s*-wave resonances.

A. Molecular state

The binding energy E_b of the molecule is given by the pole of T. In the limit $\delta \sim \delta_0$, it is therefore given by

$$E_b = \tilde\delta - i\hbar\gamma(\tilde\delta)/2,$$

We see that the real part of E_b (the "physical" binding energy) is $\sim\tilde\delta$ and therefore scales linearly with the detuning $\delta - \delta_0$. This scaling is very different from what happens for *s*-wave processes where we expect a $(\delta - \delta_0)^2$ behavior. This difference is in practice very important: indeed, the molecules can be trapped after their formation only if their binding energy is smaller than the trap depth. The scaling we get for the *p*-wave molecules means that the binding energy increases much faster when we increase the detuning than what we obtain for *s*-wave molecules (this feature was already pointed out in [11]). Hence, *p*-wave molecules must be looked for only in the close vicinity of the Feshbach resonance—for instance, for $\eta \ll 1$ (relevant for ^{6}Li, as we show below) and a trap depth of 100 μK, the maximum detuning at which molecules can be trapped is $\simeq 0.1$ G.

This asymptotic behavior of the binding energy is closely related to the internal structure of the molecule. Indeed, the molecular wave function $|\psi_m(B)\rangle$ can be written as a sum $|\text{open}\rangle + |\text{closed}\rangle$ of its projections on the closed and open channels, which correspond, respectively, to short- and long-range molecular states. If we neglect decay processes by setting $\lambda_2 = 0$, we can define the magnetic moment of the molecule (relative to that of the free atom pair) by

$$\Delta\mu_{\text{eff}}(B) = -\frac{\partial E_b}{\partial B} = -\frac{\partial\widetilde{\delta}}{\partial B},$$

that is, in the case of ^{6}Li where $\delta = 2\mu_B(B - B_0)$,

$$\Delta\mu_{\text{eff}}(B) = -\frac{2\mu_B}{1 + \eta}. \tag{8}$$

On the other hand, we can also write $E_b = \langle\psi_m(B)|\widehat{H}(B)|\psi_m(B)\rangle$. Since in the absence of any decay channel, the molecular state is the ground state of the two-body system, we can write using the Hellmann-Feynman relation

$$\Delta\mu_{\text{eff}} = -\frac{\partial E_b}{\partial B} = -\langle\psi_m(B)|\frac{\partial\widehat{H}(B)}{\partial B}|\psi_m(B)\rangle.$$

In our model, the only term of the Hamiltonian depending on the magnetic field is the energy $\delta = 2\mu_B(B - B_0)$ of the bare molecular state in the closed channel and we finally have

$$\Delta\mu_{\text{eff}} = -2\mu_B\langle\text{closed}|\text{closed}\rangle. \tag{9}$$

If we compare Eqs. (8) and (9), we see that the probability $P_{\text{closed}} = \langle\text{closed}|\text{closed}\rangle$ to be in the closed channel is given by

$$P_{\text{closed}} = 1/(1 + \eta).$$

In other words, unless $\eta = \infty$, there is always a finite fraction of the wave function in the tightly bound state. In practice, we will see that in the case of ^{6}Li, $\eta \ll 1$. This means that the molecular states that are nucleated close to a Feshbach resonance are essentially short-range molecules. On the contrary, for *s*-wave molecules, $E_b \propto (\delta - \delta_0)^2$ leads to $\Delta\mu_{\text{eff}} = -2\mu_B\langle\text{closed}|\text{closed}\rangle \propto (\delta - \delta_0)$. This scaling leads to a zero probability of occupying the bare molecular state near an *s*-wave resonance.

We can illustrate these different behaviors in the simplified picture of Fig. 3. For small detunings around threshold, the *p*-wave potential barrier provides a large forbidden region, which confines the bound state behind this barrier. The bound-state wave function decays exponentially inside the barrier and the tunneling remains nearly negligible. Since there is no significant difference for the shape of the *p*-wave bound state for small positive and negative detunings, the linear dependence of the closed channel on magnetic field will be conserved for the bound state, and therefore the binding energy will also linearly approach the threshold. We note that the linear dependence close to threshold can also be found from the general Breit-Wigner expression for a resonance, in combination with the *p*-wave threshold behavior of the phase shift [13].

The imaginary part of E_b corresponds to the lifetime of the molecule. In the case of *s*-wave molecules for which two-body decay is forbidden [20,21], the only source of instability is the coupling with the continuum of the incoming channel that leads to a spontaneous decay when $\widetilde{\delta} > 0$ [see Fig. 3(a)]. By contrast, we get a finite lifetime in the *p* wave even at $\widetilde{\delta} < 0$: due to dipolar relaxation between its constituents, the molecule can indeed spontaneously decay toward
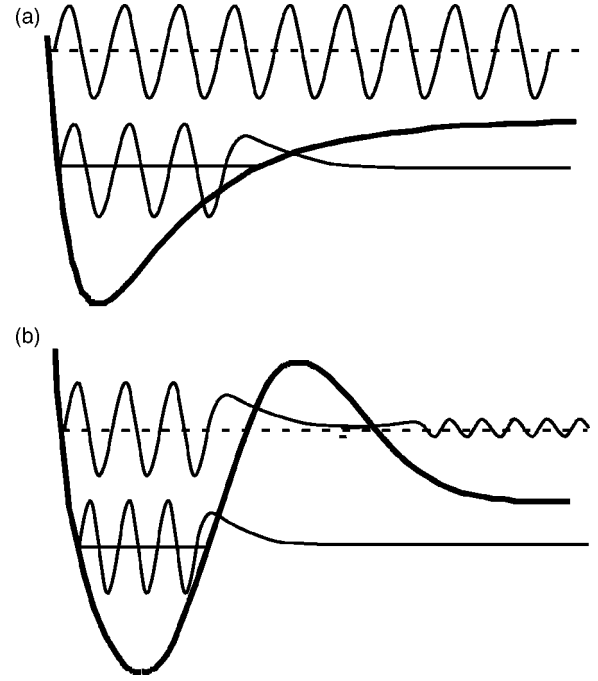

FIG. 3. Effect of the centrifugal barrier on the bound state in *p*-wave Feshbach resonances. (a) Case of *s*-wave scattering: the bare molecular state goes from $\delta < 0$ (full line) to $\delta > 0$ (dashed line). In the process, the molecular state becomes unstable and the wave function becomes unbounded. (b) In the case of a *p*-wave bound state, the presence of the centrifugal barrier smooths the transition from $\delta > 0$ to $\delta < 0$. Even for $\delta > 0$, the wave function stays located close to the bottom of the well.

state $|2\rangle$. For $\widetilde{\delta} \sim 0$, the decay rate γ_0 associated with this process is given by

$$\gamma_0 = \gamma(0) = \frac{\lambda_2}{1 + \eta}\frac{m}{3\pi\hbar^3}\left(\frac{m\Delta}{\hbar^2}\right)^{3/2}.$$

B. Elastic scattering

The scattering amplitude $f(\mathbf{k}, \mathbf{k}')$ for atoms colliding in the channel 1 can be extracted from the *T* matrix using the relation

$$f(\mathbf{k}, \mathbf{k}') = -\frac{mL^3}{4\pi\hbar^2}T_{11}(\mathbf{k}, \mathbf{k}', E = \hbar^2 k^2/m),$$

that is,

$$f(\mathbf{k}, \mathbf{k}') = -\frac{m\lambda_1}{4\pi\hbar^2}\left(\frac{k^2\cos(\widehat{\mathbf{k}, \mathbf{k}'})/(1 + \eta)}{\hbar^2 k^2/m - \widetilde{\delta} - i\hbar\gamma/2}\right).$$

The $\cos(\widehat{\mathbf{k}, \mathbf{k}'})$ dependence is characteristic of *p*-wave processes and, once again, this expression shows dramatic differences from the *s*-wave behavior. First, at low k, $f(\mathbf{k}, \mathbf{k}')$ vanishes like k^2. If we introduce the so-called scattering volume V_s [13] defined by

$$f(\mathbf{k}, \mathbf{k}') = -V_s k^2,$$

then we have

$$V_s = \frac{-m\lambda_1}{4\pi\hbar^2[\delta - \delta_0 + i(1+\eta)\hbar\gamma_0/2]} \sim \frac{-m\lambda_1}{2\pi\hbar^2(\delta - \delta_0)},$$

if we neglect the spontaneous decay of the molecule. We see that in this approximation, the binding energy E_b of the molecule is given by

$$E_b = -\frac{m\lambda_1}{2\pi\hbar^2(1+\eta)} \frac{1}{V_s}.$$

In s-wave processes, the binding energy and the scattering length are related through the universal formula $E_b = -\hbar^2/ma^2$. This relationship is of great importance since it allows one to describe both scattering properties and the molecular state with only one scattering length, without having to be concerned care with any other detail of the interatomic potential. In the case of the p wave, we see that no such universal relation exists between the scattering volume and E_b, a consequence of the fact that we have to deal with short-range molecular states, even at resonance. We therefore need two independent parameters to describe both the bound states and the scattering properties.

In the general case, the elastic cross section σ_{el} is proportional to $|f|^2$. According to our calculation, we can put σ_{el} under the general form

$$\sigma_{\mathrm{el}}(E) = \frac{CE^2}{(E - \tilde{\delta})^2 + \hbar^2\gamma^2/4}, \tag{10}$$

where $E = \hbar^2 k^2/m$ is the kinetic energy of the relative motion and C is a constant depending on the microscopic details of the system. Noticeably, the energy dependence of the cross section exhibits a resonant behavior at $E = \tilde{\delta}$ as well as a plateau when $E \to \infty$, two features that were observed in the numerical coupled-channel calculations presented in [17]. Once again, this leads to physical processes very different from what is expected in s-wave scattering. Indeed, we know that in s-wave scattering, we have $f \sim -a$, as long as $ka \ll 1$. Since a is in general nonzero, the low-energy behavior gives a non-negligible contribution to the scattering processes. By contrast, we have just seen that in the case of the p wave, the low-energy contribution is vanishingly small ($\sigma_{\mathrm{el}} \sim E^2$) so that the scattering will be dominated by the resonant peak $E \sim \tilde{\delta}$.

C. Inelastic scattering.

For two particules colliding in channel 1 with an energy $E = \hbar^2 k^2/m$, the probability to decay to channel 2 is proportional to $\rho_2(k')|T_{12}(\mathbf{k}, \mathbf{k}', E)|^2$ where ρ_2 is the density of states in channel 2. Since k' is given by the energy conservation condition $\hbar^2 k'^2/m - \Delta = E$, and in practice $\Delta \gg E$, we see that $k' \sim \sqrt{m\Delta/\hbar^2}$ is therefore a constant. Using this approximation, we can write the two-body loss rate $g_2(E)$ for particles of energy E as
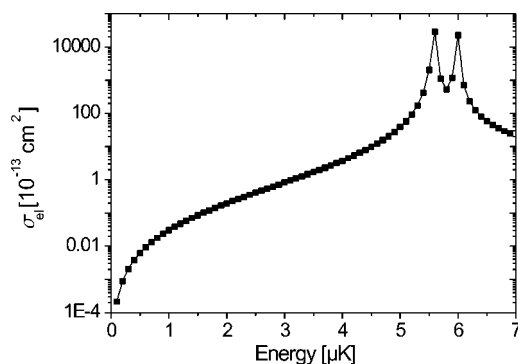

FIG. 4. Energy dependence of the elastic cross section. Dots: numerical closed-channel calculation. The left peak corresponds to $m_l = 0$ and the right peak to $m_l = \pm 1$. Full line: Fits using Eq. (11).

$$g_2(E) = \frac{DE}{(E - \tilde{\delta})^2 + \hbar^2\gamma^2/4},$$

where D is a constant encapsulating the microscopic details of the potential.

V. COMPARISON WITH COUPLED-CHANNEL CALCULATION

The quantities such as C, D, γ_0, etc., that were introduced in the previous section were only phenomenological parameters to which we need to attribute some value to be able to perform any comparison with the experiment. These data are provided by *ab initio* numerical calculations using the coupled-channel scheme described in [18]. The result of this calculation for the elastic scattering cross section is presented in Fig. 4. The most striking feature of this figure is that it displays two peaks instead of one, as predicted by Eq. (10). This difference can be easily understood by noting that the dipolar interaction that couples the molecular state to the outgoing channel provides a "spin-orbit" coupling that modifies the relative orbital angular momentum of the pair [17]. In other words, each resonance corresponds to a different value of the relative angular momentum m_l (the $m_l = +1$ and $m_l = -1$ resonances are superimposed because the frequency shift induced by the dipolar coupling is proportional to m_l^2, as noted in [17]).

As the spin-orbit coupling is not included in our simplified three-level model, we take the multiple peak-structure into account by fitting the data of Fig. 4 using a sum of three laws (10) with a different set of phenomenological parameters for each value of the angular momentum:

$$\sigma_{\mathrm{el}}(E) = \sum_{m_l=-1}^{+1} \frac{C_{m_l} E^2}{(E - \tilde{\delta}_{m_l})^2 + \hbar^2\gamma_{m_l}^2/4}, \tag{11}$$

where $\tilde{\delta}_{m_l}$ is related to the magnetic field through $\tilde{\delta}_{m_l} = \mu(B - B_{F, m_l})$ and $\gamma_{m_l} = \gamma_{0, m_l} + a_{m_l} E^{3/2}$. Using this law, we obtain a perfect fit to the elastic as well as inelastic data obtained from the coupled-channel calculations. The values obtained

TABLE I. Values of the phenomenological parameters obtained after a fit to the coupled-channel calculation data of Fig. 4. δB_F is the shift between the $m_l = \pm 1$ and $m_l = 0$ resonances.

Channel	(1/2, −1/2)			(−1/2, −1/2)		
m_l	−1	0	1	−1	0	1
$C(10^{-13}\ \text{cm}^2)$	0.22	0.22	0.22	0.87	0.88	0.87
$D(10^{-13}\ \text{cm}^2\ \mu\text{K/s})$	0.00002	0.59	0.56	3×10^{-5}	1.54	5.72
$\gamma_0(\text{s}^{-1})$	$<10^{-2}$	110	110	<1	220	830
$a(\mu\text{K}^{-1/2})$	0.0017	0.0017	0.0017	0.0024	0.0024	0.0024
η	0.22	0.22	0.22	0.23	0.23	0.23
$\delta B_F(\text{G})$	−0.0036	0	−0.0036	−0.012	0	−0.012

for the different phenomenological parameters are presented on Table I.

From these data, we see first that the "elastic" properties are independent of m_l. This comes from the fact that the elastic scattering is mainly a consequence of the hyperfine coupling that does not act on the center-of-mass motion of the atoms. However, we see that both the inelastic collision rate constant D and the molecule lifetime γ_0 exhibit large variations with the relative angular momentum [22]. First, the spontaneous decay rate γ_0 of a molecule in $m_l = 0, +1$ is always larger than $\sim 10^2\ \text{s}^{-1}$, which corresponds to a maximum lifetime of about 10 ms. Second, we observe a strong reduction of the losses in the $m_l = -1$ channel, in which no significant spontaneous decay could be found. An estimate of γ_0 can nevertheless be obtained by noting that, since the elastic parameters are independent of m_l, the ratio D/γ_0 should not depend on m_l [this can be checked by comparing the ratios D/γ_0 for $m_l = 0$ and $m_l = +1$ in the $(-1/2, -1/2)$ channel]. Using this assumption we find that $\gamma_0 \sim 4 \times 10^{-3}\ \text{s}^{-1}$ both in $(1/2, -1/2)$ and $(-1/2, -1/2)$. The reason for this strong increase of the lifetime of the molecules in $m_l = -1$ is probably because, due to angular momentum conservation, the outgoing pair is expected to occupy a state with $l = 3$ after an inelastic process. Indeed, if we start in a two-body state (m_F, m_F') and if the dipolar relaxation flips the spin m_F', then the atom pair ends up in a state $(m_F, m_F' + 1)$. This increase of the total spin of the pair must be compensated by a decrease of the relative angular momentum. Therefore, if the molecule was associated with a relative angular momentum m_l, it should end up with $m_l - 1$. In the case of $m_l = -1$, this means that the final value of the relative angular momentum is $m_l = -2$, i.e., $l \geq 2$. But, according to selection rules associated with spin-spin coupling, the dipolar interaction can only change l by 0 or 2. Therefore, starting from a p-wave ($l = 1$) compound, this can only lead to $l = 3$. Let us now assume that the coupling between the molecular state and the outgoing channel is still proportional to the overlap between the two states [see Eq. (1)], even in the presence of a dipolar coupling: the argument above indicates that the ratio $\rho = \gamma_{0, m_l = -1}/\gamma_{0, m_l' \neq -1}$ between the decay rate of molecules in $m_l = -1$ and the one of molecules in $m_l' \neq 1$ is then of the order of

$$\rho \sim \left| \frac{\int g^*(r) j_3(kr) r^2 dr}{\int g^*(r) j_1(kr) r^2 dr} \right|^2,$$

where $k = \sqrt{m\Delta/\hbar^2}$ is the relative momentum of the atoms after the decay. For lithium, we have $R_e \sim 3$ Å [23] which yields $kR_e \sim 7 \times 10^{-2}$. This permits us to approximate the spherical Bessel functions j_l by their expansion at low k, $j_l(kr) \sim (kr)^l$, that is,

$$\rho \sim k^4 \left| \frac{\int g^*(r) r^5 dr}{\int g^*(r) r^3 dr} \right|^2 \sim (kR_e)^4.$$

With the numerical value obtained for kR_e, we get $\rho \sim 2 \times 10^{-5}$, which is, qualitatively, in agreement with the numerical coupled-channel calculations presented above.

VI. TEMPERATURE AVERAGING

In realistic conditions, the two-body loss rate G_2 needs to be averaged over the thermal distribution of atoms. G_2 is therefore simply given by

$$G_2(E) = \sqrt{\frac{\pi}{4(k_B T)^3}} \int_0^\infty g_2(E) e^{-E/k_B T} E^{1/2} dE.$$

The evolution of G_2 vs detuning is displayed in Fig. 5 and shows a strongly asymmetric profile that was already noticed in previous theoretical and experimental papers [8,10].

This feature can readily be explained by noting that in situations relevant to experiments, γ_0 is small with respect to temperature. We can therefore replace g_2 by a sum of Dirac functions centered on δ_{0,m_l}. When the δ_{0,m_l} are positive, G_2 takes the simplified form

$$G_2 = 4\sqrt{\pi} \sum_{m_l} \left(\frac{D_{m_l}}{\hbar \gamma_{m_l}(\tilde{\delta}_{m_l})} \right) \left(\frac{\tilde{\delta}_{m_l}}{k_B T} \right)^{3/2} e^{-\tilde{\delta}_{m_l}/k_B T}.$$

Moreover, if we neglect the lift of degeneracy due to the dipolar interaction coupling and we assume all the $\tilde{\delta}_{m_l}$ to be equal to some $\tilde{\delta}$, we get
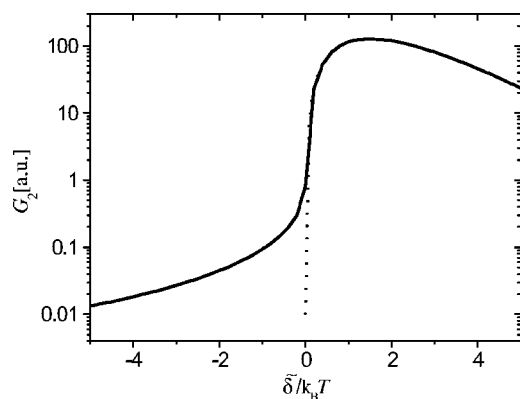
FIG. 5. Full line: numerical calculation of the loss rate for $T = 10 \ \mu K$. Dotted line: asymptotic expansion (12).

$$G_2 = 4\sqrt{\pi}\left(\frac{\bar{D}}{\hbar\,\bar{\gamma}(\tilde{\delta})}\right)\left(\frac{\tilde{\delta}}{k_BT}\right)^{3/2} e^{-\tilde{\delta}/k_BT}, \qquad (12)$$

with $\bar{D} = \Sigma_{m_l} D_{m_l}$ and $\bar{D}/\bar{\gamma} = \Sigma_{m_l} D_{m_l}/\gamma_{m_l}$ [19].

For $\tilde{\delta} < 0$ and $|\tilde{\delta}| \gg k_BT$, we can replace the denominator of g_2 by $\tilde{\delta}^2$ and we get the asymptotic form for G_2

$$G_2 = \frac{3}{2}k_BT\sum_{m_l}\frac{D_{m_l}}{\tilde{\delta}_{m_l}^2}. \qquad (13)$$

Let us now comment on the two equations (12) and (13) .

(1) We note that the maximum value of G_2 is obtained for $\tilde{\delta}/k_BT = 3/2$. It means that when tuning the magnetic field (i.e., $\tilde{\delta}$), the maximum losses are not obtained at the resonance $\tilde{\delta} = 0$, but at a higher field, corresponding to $\tilde{\delta} = 3k_BT/2$. For a typical experimental temperature $T = 10 \ \mu K$, this corresponds to a shift of about 0.1 G.

(2) Similarly, the width of $G_2(\tilde{\delta})$ scales like k_BT. Expressed in terms of magnetic field, this corresponds to ~ 0.1 G for $T = 10 \ \mu K$. This width is a consequence of the resonance nature of the scattering in p-wave processes. As seen earlier, both elastic and inelastic collisions are more favorable when the relative energy $E = \tilde{\delta}$. When $\tilde{\delta} < 0$, the resonance conditions cannot be satisfied, since there are no states in the incoming channel with negative energy. The

scattering is then formally analogous to optical pumping or other second-order processes and yields the $1/\tilde{\delta}^2$ obtained in Eq. (13). When $\tilde{\delta} \gg k_BT$, the resonance condition is satisfied by states that are not populated (since for a thermal distribution, we populate states up to $E \sim k_BT$).

VII. CONCLUSION

In this paper, we have developed a simple model capturing the main scattering properties close to a p-wave Feshbach resonance. The analytical formulas we obtained show very good agreement with both numerical coupled-channel calculations and experimental measurements from our group [9] and from Chin and Grimm [24]. We have shown that the line shape of the resonance is very different from what is expected for an s-wave process: while s-wave scattering is mainly dominated by low-energy processes, p-wave scattering is rather dominated by collisions at energies equal to that of the molecular state. Regarding p-wave molecules, we have seen that at resonance their wave function was dominated by the short-range bare molecular state. Finally, the study of the spontaneous decay of these molecules has shown a very different lifetime depending on the relative angular momentum of its constituents, since molecules in $m_l = -1$ could live 10^4 times longer than those in $m_l = 0, +1$. This very intriguing result might prove to be a valuable asset for the experimental study of p-wave molecules since it guarantees that $m_l = -1$ dimers are very stable against two-body losses in the absence of depolarizing collisions.

[1] S. Jochim, M. Bartenstein, A. Altmeyer, G. Hendl, S. Riedl, C. Chin, J. Hecker Denschlag, and R. Grimm, Science **302**, 2101 (2003).

[2] M. W. Zwierlein, C. A. Stan, C. H. Schunck, S. M. F. Raupach, S. Gupta, Z. Hadzibabic, and W. Ketterle, Phys. Rev. Lett. **91**, 250401 (2003).

[3] T. Bourdel, L. Khaykovich, J. Cubizolles, J. Zhang, F. Chevy, M. Teichmann, L. Tarruell, S. J. J. M. F. Kokkelmans, and C. Salomon, Phys. Rev. Lett. **93**, 050401 (2004).

[4] J. Kinast, S. L. Hemmer, M. E. Gehm, A. Turlapov, and J. E. Thomas, Phys. Rev. Lett. **92**, 150402 (2004).

[5] M. Greiner, C. A. Regal, and D. S. Jin, Nature (London) **426**, 537 (2003).

[6] D. M. Lee, Rev. Mod. Phys. **69**, 645 (1997).

[7] C. C. Tsuei and J. R. Kirtley, Phys. Rev. Lett. **85**, 182 (2000).

[8] C. A. Regal *et al.*, Phys. Rev. Lett. **90**, 053201 (2003).

[9] J. Zhang, E. G. M. van Kempen, T. Bourdel, L. Khaykovich, J. Cubizolles, F. Chevy, M. Teichmann, L. Tarruell, S. J. J. M. F. Kokkelmans, and C. Salomon, Phys. Rev. A **70**, 030702(R) (2004).

[10] C. H. Schunck, M. W. Zwierlein, C. A. Stan, S. M. F. Raupach, W. Ketterle, A. Simoni, E. Tiesinga, C. J. Williams, and P. S. Julienne, e-print cond-mat/0407373.

[11] T. L. Ho and N. Zahariev, e-print cond-mat/0408469; T. L. Ho and R. B. Diener, e-print cond-mat/0408468.

[12] Y. Ohashi, e-print cond-mat/0410516.

[13] J. R. Taylor, *Scattering Theory* (John Wiley, New York, 1972); H. Feshbach, *Theoretical Nuclear Physics* (John Wiley, New York, 1992).

[14] C. Chin, V. Vuletic, A. J. Kerman, and S. Chu, Phys. Rev. Lett. **85**, 2717 (2000); P. J. Leo, C. J. Williams, and P. S. Julienne, *ibid.* **85**, 2721 (2000).

[15] Thomas Volz, Stephan Drr, Niels Syassen, Gerhard Rempe, Eric van Kempen, and Servaas Kokkelmans, e-print cond-mat/0410083.

[16] A. R. Edmunds, *Angular Momentum in Quantum Mechanics* (Princeton University Princeton, NJ, Press, 1996).

[17] C. Ticknor, C. A. Regal, D. S. Jin, and J. L. Bohn, Phys. Rev. A **69**, 042712 (2004).

[18] E. G. M. van Kempen, B. Marcelis, and S. J. J. M. F. Kokkelmans, e-print cond-mat/0406722.

[19] For the sake of simplicity, these averaged parameters only were presented in [9].

[20] K. Dieckmann, C. A. Stan, S. Gupta, Z. Hadzibabic, C. H. Schunck, and W. Ketterle, Phys. Rev. Lett. **89**, 203201 (2002).

[21] H. T. C. Stoof, J. M. V. A. Koelman, and B. J. Verhaar, Phys. Rev. B **38**, 4688 (1988).

[22] Note that the different lifetimes calculated for the three m_l states do not violate any rotational symmetry. Indeed, the magnetic field used to reach the Feshbach resonance provides a preferred direction to the system.

[23] We evaluate R_e by identifying it with the relative distance r at which the total (centrifugal + long-range) potential $3\hbar^2/mr^2 - C_6/r^6 - C_8/r^8 - C_{10}/r^{10}$ cancels and we used the $C_{8,9,10}$ coefficients of [24]. Z.-C. Yan *et al.*, Phys. Rev. A **54**, 2824 (1996).

[24] C. Chin and R. Grimm (private communication).